Differential action of steroid hormones on human endothelium

Hans Oberleithner[1,*], Christoph Riethmüller[1], Thomas Ludwig[1], Victor Shahin[1], Christian Stock[1], Albrecht Schwab[1], Martin Hausberg[2], Kristina Kusche[3] and Hermann Schillers[1]

[1]Institute of Physiology II, [2]Department of Internal Medicine D and [3]Institute of Zoophysiology, University Münster, 48149 Münster, Germany

*Author for correspondence (e-mail: oberlei@uni-muenster.de)

Accepted 11 January 2006
Journal of Cell Science 119, 1926-1932 Published by The Company of Biologists 2006
doi:10.1242/jcs.02886

Summary

The action of glucocorticoids on vascular permeability is well established. However, little is known about the action of mineralocorticoids on the structure and function of blood vessels. As endothelial cells are targets for both glucocorticoids and mineralocorticoids, we exposed human umbilical vein endothelial cells to both types of steroids. Aldosterone (mineralocorticoid) and dexamethasone (glucocorticoid) were applied for 3 days in culture before measurements of transendothelial ion and macromolecule permeability, apical cell surface and cell stiffness were taken. Transendothelial ion permeability was measured with electrical cell impedance sensing, macromolecule permeability with fluorescence-labeled dextran and apical cell membrane surface by three-dimensional AFM imaging. Cell stiffness was measured using the AFM scanning tip as a mechanical nanosensor. We found that aldosterone increased both apical cell surface and apical cell stiffness significantly, while transendothelial permeability remained unaffected. By contrast, dexamethasone significantly decreased ion and macromolecule permeability, while apical cell surface and cell stiffness did not change. Specific receptor antagonists for dexamethasone (RU486) and aldosterone (spironolactone) prevented the observed responses. We conclude that glucocorticoids strengthen cell-to-cell contacts ('peripheral action'), whereas mineralocorticoids enlarge and stiffen cells ('central action'). This could explain the dexamethasone-mediated retention of fluid in the vascular system, and endothelial dysfunction in states of hyperaldosteronism.

Key words: Atomic force microscopy, Mineralocorticoid, Endothelial permeability, Endothelial cell surface, Spironolactone, Cell stiffness, Epithelial sodium channel

Introduction

Although the action of glucocorticoids is known to be widespread in humans, mineralocorticoid action is thought to be more organ specific. The major mineralocorticoid hormone, aldosterone, is synthesized in the zona glomerulosa of the adrenal cortex, and is secreted in small amounts (150 μg daily) in response to a fall in blood pressure and extracellular volume. The kidney is known to be the main target for aldosterone, where it acts upon electrolyte transport in the distal nephron (Robert-Nicoud et al., 2001). However, aldosterone acts not only on epithelial cells of the kidney and colon, but also on non-epithelial sites in the brain, heart and vasculature (Connell and Davies, 2005). The hormone exerts genomic and non-genomic actions, and usually involves the classical intracellular receptors for intracellular signalling (Funder, 2005). A growing number of studies indicate that aldosterone plays a potentially crucial role in the development of heart failure, myocardial fibrosis and endothelial dysfunction (Stier, Jr et al., 2002). This view has triggered much interest in the use of aldosterone receptor blockade in patients to diminish the pathological effects that can be produced by this hormone (Palmieri et al., 2002).

Although there is increasing excitement about the use of new aldosterone inhibitors (Pitt et al., 2003) in the treatment of cardiovascular disease, little is known about how aldosterone acts on heart and blood vessels from the physiological point of view. Glucocorticoids are known to decrease transendothelial fluid flow (Underwood et al., 1999), to upregulate occludin expression, a major protein of intercellular junctions (Forster et al., 2005), to increase transendothelial electrical resistance (Cucullo et al., 2004), and to reduce paracellular permeability for macromolecules (Romero et al., 2003). In the latter study, dexamethasone treatment led to the accumulation of actin-binding proteins associated with filamentous actin at the periphery of rat brain endothelial cells. Taken together, glucocorticoids clearly act on intercellular junctions. In contrast to the wealth of information concerning glucocorticoid action on endothelium, knowledge of the action of aldosterone upon endothelium is rather poor. It is not known whether aldosterone plays a regulatory role in transendothelial permeability. So far, the development of a model of how endothelial cells could function in response to aldosterone has been hindered by the limited amount of experimental data. Endothelial cells display considerable phenotypic heterogeneity, making it difficult to choose the 'most adequate' cell system (Minami and Aird, 2005). Among them, human umbilical vein endothelial cells (HUVEC) could serve as a suitable cell system for aldosterone action in vitro for several reasons: (1) HUVEC maintain the major characteristics of endothelial cells in primary culture (Muller et al., 2002); (2)

they express mineralocorticoid receptors (Lombes et al., 1992; Oberleithner et al., 2003) and aldosterone-sensitive epithelial sodium channels (Golestaneh et al., 2001); and (3) they respond to aldosterone via non-genomic and genomic pathways (Oberleithner et al., 2003; Oberleithner et al., 2004). As the umbilical vein carries arterial blood from the placenta to the foetus at moderate hydrostatic pressure, HUVEC are exposed to conditions in vivo similar to those of endothelial cells in small arterial blood vessels. For these reasons, we chose HUVEC as a cell model system with which to study the effects, in vitro, of aldosterone on apical membrane topography and transendothelial permeability for ions and macromolecules, compared with those of glucocorticoids. By means of atomic force microscopy (AFM), a nanotechnique (Binnig and Quate, 1986) that allows the measurement of apical endothelial cell surface and stiffness, we addressed the issue of aldosterone-induced structural and functional remodeling of the endothelium. From previous experiments, we knew that HUVEC swell in response to aldosterone owing to the activation of apical sodium channels (Oberleithner et al., 2004). In the present study, experiments with the synthetic glucocorticoid dexamethasone served as reference measurements to evaluate steroid specificity and to distinguish between gluco- and mineralocorticoid action in endothelium. Our results support the view that glucocorticoids regulate intercellular junctions and thus determine paracellular permeability, while, in contrast, aldosterone lacks such effects but decreases cell elasticity.

Results

Endothelial cells, grown to confluence and cautiously fixed under physiological conditions, were scanned in liquid and cell surfaces were calculated. Fig. 1 shows three representative AFM images obtained under different conditions. HUVEC maintained an 'in vivo' shape and volume during fixation and AFM scanning in fluid (Schneider et al., 2004). As summarized in Fig. 2, there is a substantial increase in the apical membrane surface of aldosterone-treated cells. This 64% increase in the apical cell surface was completely blocked by spironolactone. In contrast to aldosterone, we could not detect any significant changes in the cell surface upon treatment with dexamethasone, or with dexamethasone and its antagonist RU486.

Due to the large increase in apical cell surface, we expected changes in mechanical cell elasticity. We therefore used AFM as a mechanosensor and measured the force necessary to vertically indent the apical membrane in live HUVEC by 300 nm. The results are summarized in Fig. 3. Prior to the treatment with aldosterone, a force of 3.08±0.4 kPa was measured. After aldosterone treatment, a loading force of 5.5±0.7 kPa was necessary (P<0.001). This increase of cell stiffness could be prevented by spironolactone. In contrast to aldosterone, and consistent with the lack of change in the cell surface, dexamethasone or dexamethasone plus its antagonist RU486 did not influence cell stiffness.

We next tested whether these dramatic aldosterone-induced changes in the HUVEC monolayer architecture were reflected by altered permeability. We applied two technical approaches. In a series of experiments, we investigated transendothelial solute permeability by using fluorescence-labeled, 40-kDa

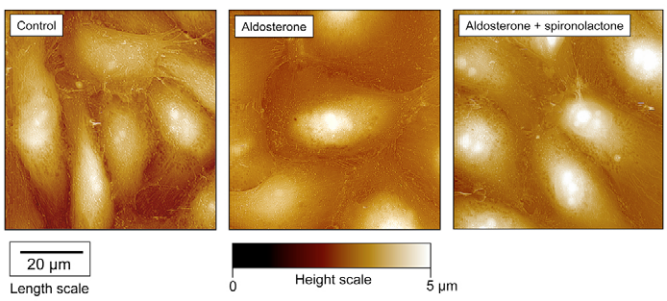

Fig. 1. AFM images of HUVEC monolayers viewed from the top. Cells were exposed for 72 hours to solvent (control), to aldosterone, or to aldosterone and spironolactone. The height bar below quantifies the height of the images.

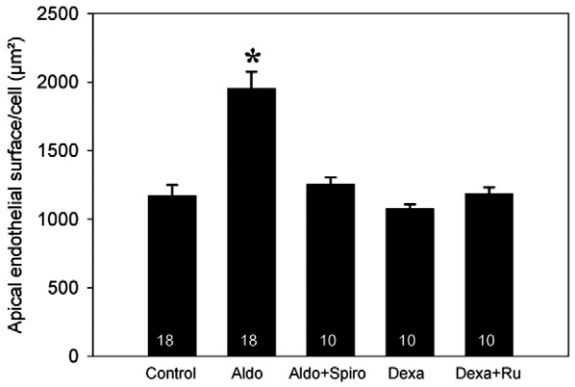

Fig. 2. Apical plasma membrane surface of individual endothelial cells (HUVEC). Cells were exposed for 72 hours to solvent (control), to aldosterone (aldo), to aldosterone and spironolactone (aldo+spiro), to dexamethasone (dexa), or to dexamethasone and RU486 (dexa+RU). Mean values ± s.e.m. are shown; the number of scans is shown in the bars, each scan represents between 7-15 cells. Asterisk indicates significant difference in comparison with control (P<0.01).

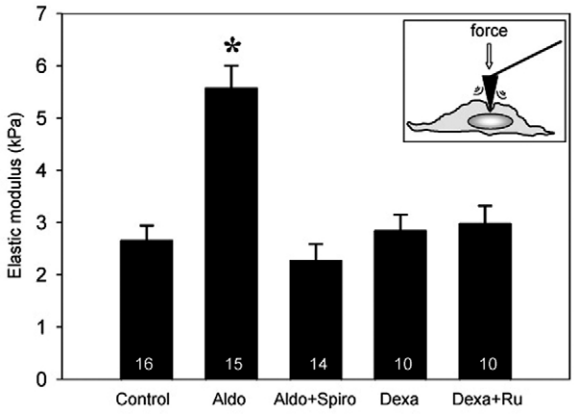

Fig. 3. Endothelial cell stiffness (elastic modulus) in living HUVEC. Cells were exposed for 72 hours to solvent (control), to aldosterone (aldo), to aldosterone and spironolactone (aldo+spiro), to dexamethasone (dexa), or to dexamethasone and RU486 (dexa+RU). Mean values ± s.e.m. are shown; the number of individual cells in which stiffness was measured is shown in the bars. Asterisk indicates significant difference in comparison with control (P<0.01).

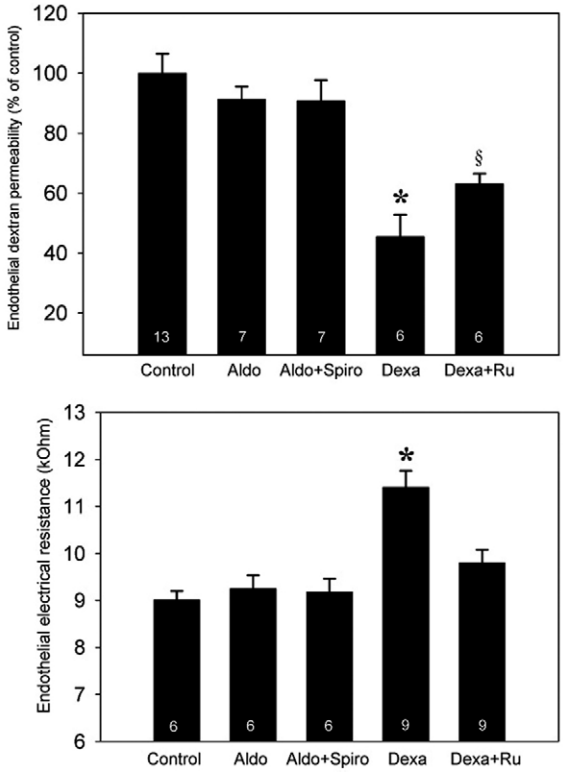

Fig. 4. (A) Transendothelial dextran permeability measured with fluorescence-labeled 40 kDa dextran. Cells were exposed for 72 hours to solvent (control), to aldosterone (aldo), to aldosterone and spironolactone (aldo+spiro), to dexamethasone (dexa), or to dexamethasone and RU486 (dexa+RU). Mean values ± s.e.m. are shown; the number of measurements on individual monolayers is shown in the bars. Asterisk indicates significant difference in comparison with control ($P<0.01$); § indicates significant difference in comparison with dexamethasone ($P<0.02$). (B) Transendothelial electrical resistance measured with the electrical cell impedance sensing (ECIS) technique. Cell treatment was as described in section A. Mean values ± s.e.m. are shown; the number of measurements on individual monolayers is shown in the bars. Asterisk indicates significant difference in comparison with control ($P<0.01$).

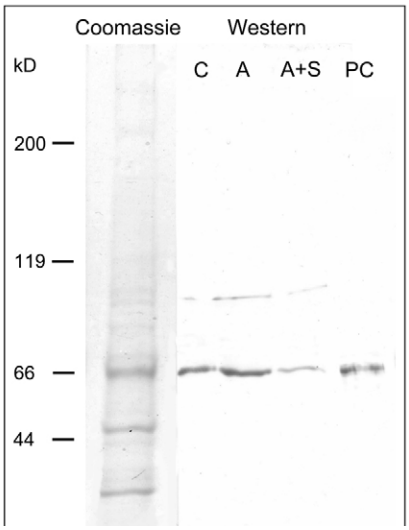

Fig. 5. Identification of αENaC in human endothelial cells (HUVEC; representative experiment). Membrane proteins were separated by SDS-PAGE and stained with Coomassie brilliant blue (lane 1). αENaC was detected by using an anti-αENaC antibody (lanes 2-4). The amount of αENaC in the aldosterone-treated sample (A) is about twice that in the control (C) and about 6 times higher than that of aldosterone and spironolactone (A+S)-incubated HUVEC. As positive control (PC), we used ENaC-expressing oocytes. The molecular mass standard is given on the left. The upper band in the range of 90 kDa most likely represents a glycosylated form of ENaC.

dextran as a flux tracer (Fig. 4A). This approach usually tests the permeability of the paracellular pathway for small macromolecules. Surprisingly, we found no significant differences in transendothelial permeability between aldosterone-stimulated and non-stimulated HUVEC monolayers. In contrast to aldosterone, dexamethasone evoked a significant decrease in endothelial permeability, which was prevented by its antagonist RU486. In another series of experiments, we investigated transendothelial electrical resistance by electrical cell impedance sensing (ECIS). This approach tests the electrical resistance of the paracellular pathway for charged ions (Fig. 4B). Again, we found no significant changes in response to aldosterone. Dexamethasone, however, significantly increased the transendothelial electrical resistance. This effect was clearly blocked by RU486. Taken together, dexamethasone affects the paracellular pathway without apparent changes in cell morphology. By contrast, aldosterone affects cell morphology without changes in paracellular permeability. This observation led us to focus more upon the cell surface properties after aldosterone exposure. Previous experiments have demonstrated that aldosterone-treated endothelium becomes sensitive to the sodium channel-blocker amiloride (Oberleithner et al., 2004). Aldosterone-induced cell swelling could be prevented by amiloride. This amiloride sensitivity indicated the functional activity of the epithelial sodium channels in HUVEC. Therefore, we attempted to show the presence of the epithelial sodium channel in the endothelium. We performed western blot analysis of the αENaC subunit in cells exposed for 72 hours to the solvent (control), to aldosterone, or to aldosterone and spironolactone. The αENaC antibody recognises a specific band with an apparent molecular mass of about 67 kDa (Fig. 5), which is the same as that reported for the αENaC subunit (Hughey et al., 2003). There was an increase in the quantity of αENaC in HUVEC incubated in aldosterone (A), when compared with cells incubated with control (C), or with aldosterone and spironolactone (A+S). These data support the view that the epithelial sodium channels in endothelium are under the control of aldosterone.

Discussion

The focus of the present study is upon steroid hormone action in endothelium. We have highlighted the actions of aldosterone because little is known about it. There appear to be three findings that warrant discussion. The first is the dramatic increase in apical cell surface. The second is the apparent lack of change in endothelial permeability. The third is the increase in cell stiffness. All three observations were made after treatment with aldosterone and were prevented by a blockade of the intracellular receptors. The effects of aldosterone on

endothelium are selective for mineralocorticoids, as the glucocorticoid dexamethasone exerts a completely different spectrum of action. Dexamethasone affects neither the endothelial cell surface nor endothelial cell stiffness. However, dexamethasone does decrease endothelial permeability, as expected (Romero et al., 2003). The reason for the selective effects of the different steroids can be explained as follows. Similar to in the kidney (Farman and Rafestin-Oblin, 2001), the mineralocorticoid receptor in endothelium (Hadoke et al., 2001) is well protected by an enzyme, 11β-hydroxysteroid dehydrogenase type 2 (HSD2). This enzyme plays a crucial role in preventing major glucocorticoid access to the mineralocorticoid receptor. HSD2 transforms glucocorticoids into metabolites that have no affinity for the mineralocorticoid receptors (Funder et al., 1988). Taken together, even high blood concentrations of glucocorticoids should not be able to mimick the selective action of aldosterone in endothelium.

The renal response to aldosterone is usually the retention of sodium and the secretion of potassium. In addition, aldosterone stimulates renal proton secretion. Target cells are the principal and intercalated cells of renal collecting ducts that thus control acid-base and electrolyte balance in the human body (Al Awqati and Schwartz, 2004). In the kidney, similar to in other organs and tissues, aldosterone exerts a transient, fast (non-genomic) response at a subcellular level that triggers a sustained, late (genomic) response resulting in modified epithelial function (Boldyreff and Wehling, 2004). A typical response to aldosterone in kidney is the recruitment of sodium channels stored in the subapical membrane vesicles of principal cells (Schafer, 2002; Palmer and Frindt, 2000). This causes sodium retention by the kidney. A similar scenario could occur in endothelial cells. Vascular endothelium expresses mineralocorticoid receptors (Lombes et al., 1992; Oberleithner et al., 2003) and epithelial sodium channels (Golestaneh et al., 2001; Chen et al., 2004) or closely related isoforms of sodium channels (Vigne et al., 1989). In the present study, western blot experiments confirm the presence of ENaC in HUVEC. In addition, they indicate that αENaC expression is increased after aldosterone treatment and is inhibited by spironolactone.

Similar to in kidney, the endothelium responds to the epithelial sodium channel blocker amiloride (Oberleithner et al., 2004). Aldosterone-induced endothelial ‘cell expansion’ could be the result of several mechanisms, one of which could be sodium entry into the cell. Owing to cell depolarisation, which naturally occurs when positively charged sodium ions diffuse into cells, diffusible chloride anions accumulate in the cell and, for osmotic reasons, expand the cell. Another reason for cell swelling (Oberleithner et al., 2004) is the intracellular accumulation of non-diffusible aldosterone-induced proteins. Such proteins could be signalling molecules, enzymes and other regulatory macromolecules, the occurrence of which is triggered by aldosterone, indicating ongoing proliferation and differentiation processes (Krug et al., 2003).

The second finding of the present study is the differential response of the two types of steroids concerning endothelial permeability. We applied two technical approaches. The electrical approach tests the ion permeability of the paracellular pathway (Wegener et al., 2000), whereas the dextran permeability approach reflects macromolecule diffusion across the endothelium (Tanaka et al., 2004). Surprisingly, the paracellular pathway for both ions and dextrans remained unaltered by aldosterone treatment, despite dramatic endothelial remodeling. This finding clearly contrasts with the well-established action of glucocorticoids, namely decreasing endothelial permeability (Romero et al., 2003).

The third finding of the present study is the substantial increase in endothelial cell stiffness in response to aldosterone and the lack of change with dexamethasone treatment. In Sprague-Dawley rats, it was previously described that aldosterone is able to increase arterial stiffness independently of wall stress (Lacolley et al., 2002). In another study, it was shown that the exposure of HUVEC to monocytes increases the deformability (i.e. decreases the stiffness) of endothelial cells (Kataoka et al., 2002). The present data show that a steroid hormone (aldosterone) can decrease the deformability (i.e. increase the stiffness) of endothelial cells. From a technical point of view, we cannot identify the increase in stiffness as being a decrease in plasma membrane elasticity, as an increase in intracellular hydrostatic or onkotic pressure, or as an aldosterone-induced strengthening of the cytoskeleton. We can only state that significantly more force is necessary to deform the first 300 nm of a cell that is about 5000 nm in height. Interestingly, dexamethasone has no influence on the deformability of the cell, indicating that, in contrast to aldosterone, the action of glucocorticoids is focused upon the intercellular junctions. This conclusion is strongly supported by studies showing the dexamethasone-induced upregulation of tight junction proteins and the accumulation of cytoskeletal proteins as filamentous actin in the cell periphery but not in the cell center (Forster et al., 2005; Romero et al., 2003).

Potential physiological relevance

The substantial change in the surface morphology of the endothelium triggered by aldosterone could have a major impact on the nitric oxide formation mediated by shear stress. It is well known that the most important stimulus for the continuous formation of NO is the viscous drag generated by the streaming blood on the endothelial layer (Davies et al., 2003; Fleming and Busse, 2003). Because endothelial cells stiffen considerably in presence of aldosterone, it is tempting to speculate that the impact of shear stress is reduced under these conditions and, thus, continuous NO production is lowered. This, in turn, could augment the mechanical tension of vascular smooth muscle and eventually increase the peripheral vascular resistance.

A ‘less deformable’ endothelial monolayer could also compromise the compliance of blood vessels and contribute to the arterial stiffness observed in high aldosterone (Lacolley et al., 2002) or high dietary sodium (Gates et al., 2004) states. In particular, pathophysiological processes could occur in small blood vessels in which the deformability of the endothelial monolayer is crucial for function.

The aldosterone-induced stiffness of endothelial cells could also be caused by the modulation of NADH/NADPH-dependent oxidases (Rajagopalan et al., 2002), and/or the nitric oxide synthase pathway (Farquharson and Struthers, 2000). Presumably, aldosterone-triggered formation of a superoxide anion, a potent scavenger of nitric oxide, could stiffen endothelial cells by as yet unknown molecular mechanisms. Furthermore, it appears that, during aldosterone exposure, a small percentage of cell borders cannot withstand the increased

mechanical forces (i.e. cell stiffness) and, therefore, develop gaps between cells (Oberleithner, 2005). Such 'non-selective' diffusion pathways could allow large proteins to pass through the endothelium and contribute to the endothelial dysfunction observed in hyperaldosteronism. Nevertheless, gaps between cells either only occur rarely or they are 'occupied' by large proteins 'in transit', as they are functionally silent in the permeability assays. Finally, we observed that the length of the intercellular borders (measured per area of monolayer surface) is significantly reduced after aldosterone treatment (data not shown). Such a reduction in length was expected, as individual cells grow in size when exposed to aldosterone. In other words, a monolayer composed of small cells has an increased total cell border length when compared with a monolayer composed of large cells. Taken together, gap formation, on the one hand, and a reduction in cell-to-cell border length, on the other, as observed after aldosterone exposure- could 'neutralise' each other, with the result that overall permeability remains unchanged. Although 'normal' paracellular diffusion and 'abnormal' diffusion through gaps obviously add up to a 'normal' overall permeability of the endothelium, it remains open to question whether the selectivity of the endothelial filter barrier is altered by aldosterone.

Materials and Methods

Endothelial cell culture and preparation for AFM

Human umbilical venous endothelial cells (HUVEC) were grown in culture as previously described (Jaffe et al., 1973; Goerge et al., 2002). In brief, cells (passage p0) were cultivated in T_{25} culture flasks coated with 0.5% gelatine (Sigma-Aldrich Chemie GmbH, Steinheim, Germany). After reaching confluence, cells were split using trypsin and then cultured (passage p1) on thin (15-mm diameter) glass coverslips coated with 0.5% gelatine and cross-linked with 2% glutaraldehyde. Glass coverslips were placed in Petri dishes filled with culture medium. HUVEC formed confluent monolayers within 72 hours (at 37°C, 5% CO_2). Chemicals were added to the medium as appropriate. Aldosterone (d-aldosterone, Sigma-Aldrich Chemie GmbH, Steinheim, Germany) was dissolved in ethanol (1 mM stock solution, stored at 4°C for two weeks). The final concentration in the experiments was 10 nM. Spironolactone (ICN Biochemicals GmbH, Eschwege, Germany) was dissolved in ethanol (1 mM stock solution) and applied at a final concentration of 100 nM. Dexamethasone (water soluble, Sigma-Aldrich Chemie GmbH, Steinheim, Germany) was dissolved in water (1 mM stock solution, stored at –20°C). Final concentration in the experiments was 100 nM. RU486 (Mifepristone; Sigma-Aldrich) was dissolved in ethanol (10 mM stock solution) and applied at a final concentration of 10 μM. After an appropriate period of time, HUVEC were exposed to glutaraldehyde (0.5% final concentration), which was gently added to the medium. This procedure crosslinks the proteins and maintains the three-dimensional structure of the cell. Because cells should maintain shape and volume as in the in vivo conditions, we designed a specific fixation procedure. (1) HUVEC were grown on glass coverslips, coated with gelatine, in an incubator perfused with 5% CO_2. (2) The coverslips were placed on the bottom of culture dishes (30-mm diameter) filled with 3 ml of culture medium. (3) Fixation was performed by adding a small volume (300 μl) of HEPES buffer, 5% glutaraldehyde to 3 ml of the medium bathing the HUVEC monolayer. (4) Fixation was performed in the CO_2 gassed incubator at 37°C. (5) After a fixation period of 60 minutes, the culture medium containing the fixative was exchanged for HEPES buffer. The samples could then be stored for days in fluid (buffer) at 4°C.

AFM apical surface measurements

The method of three-dimensional imaging by AFM has been described in detail (Henderson et al., 1996; Schneider et al., 2004; Pfister et al., 2005; Bozec and Horton, 2005). Briefly, AFM was performed in fluid using a Nanoscope III Multimode-AFM (Digital Instruments, Santa Barbara, California, USA) with a J-type scanner (maximal scan area was 100×100 μm). V-shaped oxide-sharpened, DNP-S gold-coated cantilevers with spring constants of 0.06 N/m (Digital Instruments) were used for scanning in fluid. In order to estimate changes in cell volume and apical cell surface due to fixation, we performed paired studies, scanning monolayers before and after adding the fixative. We scanned living cells in HEPES buffer at 37°C, measuring cell volume (Oberleithner et al., 2003) and apical cell surface (see below). In 14 scans (each scan being 100×100 μm), we measured a volume per cell of 1605±63 fl in vivo and 1788±54 fl after fixation (P<0.05; paired comparison), and an apical surface per cell of 1209±24 μm^2 in vivo and 1307±32 μm^2 after fixation (P<0.05; paired comparison). Images are shown in Fig. 6. The small but significant differences in cell volume and surface before and after fixation is explained by the different cell deformability caused by the AFM tip under the two conditions. A living cell is more deformable than a fixed one, and thus volume and surface are rather underestimated. Therefore, the absolute values obtained under fixed conditions are most likely closer to the real in vivo situation.

Apical membrane area was calculated as follows: surface profiles (512×512 pixels) of apical membranes were obtained from 100×100 μm images. It follows that 262,144 pixels were available to resolve these images, which contain about 7 to 15 cells, depending upon the experimental conditions. In other words, about 26 pixels were available to resolve a surface area of 1 μm^2. Image analysis was carried out using the 'roughness' feature of NanoScope III software (Digital Instruments). This software tool calculates the absolute surface of an image, including x, y and z information. A mean apical cell surface (in μm^2) was obtained by dividing the total apical monolayer surface by the number of cells.

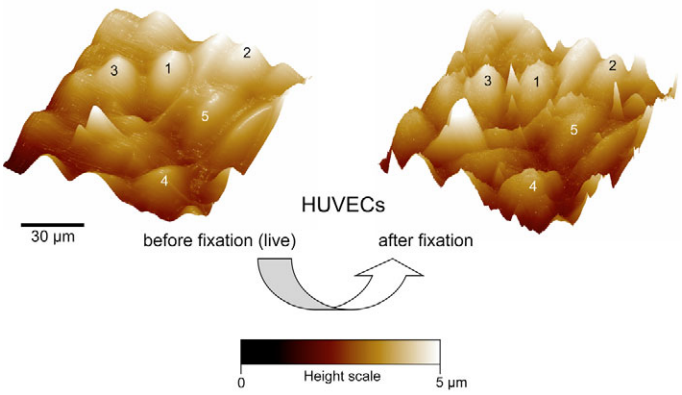

Fig. 6. Comparison between measurements in human endothelial cells (HUVEC) before and after fixation (paired experiment). (Left) AFM image showing a HUVEC monolayer scanned in vivo in HEPES buffer at 37°C. (Right) AFM image showing the same monolayer after glutaraldehyde fixation. Numbers in images indicate corresponding cells.

AFM apical elasticity measurements

Measurements of the elastic modulus termed 'cell stiffness' in this paper (a term that includes the elastic properties of the cell membrane and of the underlying cellular components) were performed with AFM, using the same equipment as described above except that softer cantilevers were used (MLCT-contact microlevers; spring constant: 0.01 N/m; Digital Instruments). Technical details have been published previously (Hoh and Schoenenberger, 1994; Oberleithner et al., 1997; Schneider et al., 2000; Schneider et al., 2004). In principle, the AFM is used as a mechanical sensor (Fig. 7). In a first step, the living HUVEC monolayer is imaged in HEPES-buffered saline. In a second step, an individual cell is selected from the image and the AFM tip is guided to the highest point of this cell (i.e. the plasma membrane above the nucleus) and the force measurement is started. The AFM tip is pressed against the cell so that the membrane is indented. At the same time, the AFM cantilever that serves as a soft spring is distorted. Force-distance curves quantify the force (N) necessary to indent the membrane for a given distance (m). The elastic (Young's) modulus was estimated using the Hertz model that describes the indentation of elastic material (Radmacher et al., 1996), and is defined as follows: $F=\delta^2\times(2/\pi)\times[E/(1-\nu^2)]\times\tan(\alpha)$, where F is the applied force (calculated from the spring constant (0.01 N/m) multiplied by the measured cantilever deflection), E is the elastic modulus (kPa), ν is the Poisson's ratio (assumed to be 0.5 because the cell was considered incompressible), α is the opening angle of the AFM tip (35°), and δ is the indentation depth (300 nm).

Repetitive force curves (5 to 10 curves obtained over a period of one minute) were obtained on individual cells and monitored online. During offline analysis slopes of individual curves were averaged. This mean value was then used as the representative force curve of a single cell.

The monolayers were prepared as described above. However, it should be emphasised that all stiffness measurements were performed in living HUVEC by applying HEPES-buffered saline. This is important because cell stiffness is significantly altered by fixatives (Hoh and Schoenenberger, 1994).

Measurement of transendothelial electrical resistance

Electrical resistance of confluent HUVEC monolayers was monitored by electrical cell impedance sensing (ECIS), a sensitive method described in detail by Giaever's group (Tiruppathi et al., 1992; Wegener et al., 2000). In brief, cells were cultivated

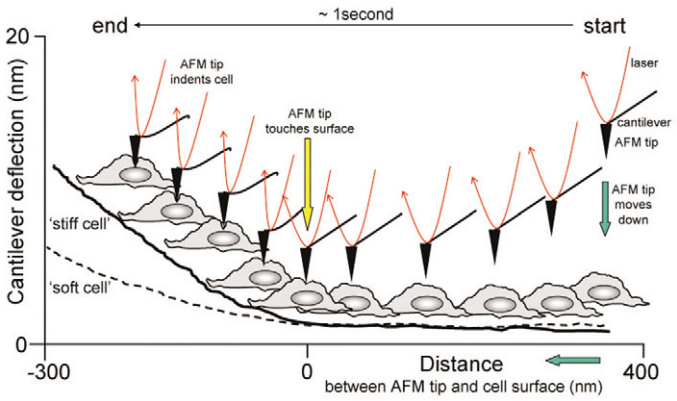

Fig. 7. Principle of cell stiffness measurements (force-distance curves) performed on living human endothelial cells with an atomic force microscope (AFM). For technical details, see Materials and Methods.

on gold electrode plates (type 8W1, electrode area 5×10^{-4} cm^2, Applied Biophysics, Troy, NY, USA) coated with fibronectin (Boehringer, Mannheim, Germany), under the conditions described above. Aldosterone, aldosterone and spironolactone, dexamethasone, dexamethasone and RU486, or solvent (control) were added at appropriate concentrations (see above). A confluent cell layer was obtained 2 days after seeding at a density of 10^5 cells/cm^2. Electrical endothelial resistance was measured 5 days after seeding using a frequency of 400 Hz. Typically, HUVEC monolayers exhibited resistances of 10±2 kOhms. Measurements were carried out in a humidified chamber supplied with 5% CO_2 at 37°C.

Determination of endothelial macromolecule permeability

The passage of FITC-labeled dextran (40 kDa average molecular mass, dialysed for 24 hours against PBS to dilute unbound FITC; Sigma, Deisenhofen, Germany) across a confluent HUVEC monolayer was measured. We applied 40 kDa dextran because macromolecules with sizes of about 4.5 nm in diameter appeared suitable to diffuse across endothelial paracellular pathways and to detect changes in free diffusion coefficients induced by the application of steroids, as previously reported (Romero et al., 2003).

Dextrans do not bind to extracellular receptors and thus are regarded as being markers of passive macromolecule transendothelial transport. Cells (2×10^5/cm^2) were seeded onto fibronectin-coated filter membrane inserts (filter area, 0.31 cm^2; pore diameter, 0.4 μm; pore density, 10^8/cm^2; Becton Dickinson, Heidelberg, Germany) and grown in medium with aldosterone, aldosterone and spironolactone, dexamethasone, dexamethasone and RU486, or solvent (control), as appropriate (see above). In order to obtain equal hydrostatic pressure, upper and lower compartments contained 400 and 1000 μl of medium, respectively. The layers reached confluence after four days, which was ascertained functionally (solute permeability) and, in selected samples, by AFM. Measurements were carried out on day five in a humidified chamber supplied with 5% CO_2, according to the following protocol. FITC-dextran (final concentration, 50 μM) was added to the upper compartment and 10 μl aliquots were taken from this compartment as a 100% reference for each filter (=maximal fluorescence). After 0, 15, 30, 45 and 60 minutes, 10 μl aliquots were collected from the lower compartment, transferred to a 96-well plate and read fluorimetrically (Fluoroskan II, Labsystems, Franklin, MA, USA). Permeability was calculated by multiple, linear regression of values relative to the initial value. To allow comparison between groups, values were normalized to the control group (100%).

Protein chemistry

Membrane proteins from HUVEC were isolated using Triton X-100 in phosphate-buffered saline. For western blotting, about 10 μg protein was submitted to SDS-PAGE (7.5% acrylamide) and transferred to a nitrocellulose membrane. Non-specific binding sites were blocked for 4 hours with 5% nonfat dry milk in Tris-buffered saline/Tween (TBST; 140 mM NaCl, 10 mM Tris-HCl, 0.3% Tween 20, pH 7.4). The epithelial sodium channel α subunit (αENaC) was detected with an anti-αENaC antibody (Dianova, Hamburg, Germany), diluted 1:5000 in 5% nonfat dry milk/TBST, overnight at 4°C. After washing in TBST, the membrane was incubated for 1 hour at room temperature with goat-anti-rabbit IgGs conjugated with alkaline phosphatase (Dianova, Hamburg, Germany), diluted 1:10,000 in 5% nonfat dry milk/TBST. The membrane was washed again in TBST and detection was carried out with nitroblue tetrazolium and 5-bromo-4-chloro-3-indolyl phosphate. A positive control was carried out with proteins isolated from ENaC-expressing oocytes.

Statistics

Data are shown as mean value ± standard error of the mean (s.e.m.). Significance of differences was evaluated by unpaired Student's *t*-test or one-way analysis of variance (ANOVA). Pairwise multiple comparison procedures performed using the Holm-Sidak method. Overall significance level was 0.05.

This study was supported by Deutsche Forschungsgemeinschaft SFB 629 A6 and DFG Re 1284/2-1. The technical support of Digital Instruments (VEECO, Mannheim) is gratefully acknowledged.

References

Al Awqati, Q. and Schwartz, G. J. (2004). A fork in the road of cell differentiation in the kidney tubule. *J. Clin. Invest.* **113**, 1528-1530.
Binnig, G. and Quate, C. F. (1986). Atomic force microscope. *Phys. Rev. Lett.* **56**, 930-934.
Boldyreff, B. and Wehling, M. (2004). Aldosterone: refreshing a slow hormone by swift action. *News Physiol. Sci.* **19**, 97-100.
Bozec, L. and Horton, M. (2005). Topography and mechanical properties of single molecules of type I collagen using atomic force microscopy. *Biophys. J.* **88**, 4223-4231.
Chen, W., Valamanesh, F., Mirshahi, T., Soria, J., Tang, R., Agarwal, M. K. and Mirshahi, M. (2004). Aldosterone signaling modifies capillary formation by human bone marrow endothelial cells. *Vascul. Pharmacol.* **40**, 269-277.
Connell, J. M. and Davies, E. (2005). The new biology of aldosterone. *J. Endocrinol.* **186**, 1-20.
Cucullo, L., Hallene, K., Dini, G., Dal, T. R. and Janigro, D. (2004). Glycerophosphoinositol and dexamethasone improve transendothelial electrical resistance in an in vitro study of the blood-brain barrier. *Brain Res.* **997**, 147-151.
Davies, P. F., Zilberberg, J. and Helmke, B. P. (2003). Spatial microstimuli in endothelial mechanosignaling. *Circ. Res.* **92**, 359-370.
Farman, N. and Rafestin-Oblin, M. E. (2001). Multiple aspects of mineralocorticoid selectivity. *Am. J. Physiol. Renal Physiol.* **280**, F181-F192.
Farquharson, C. A. and Struthers, A. D. (2000). Spironolactone increases nitric oxide bioactivity, improves endothelial vasodilator dysfunction, and suppresses vascular angiotensin I/angiotensin II conversion in patients with chronic heart failure. *Circulation* **101**, 594-597.
Fleming, I. and Busse, R. (2003). Molecular mechanisms involved in the regulation of the endothelial nitric oxide synthase. *Am. J. Physiol. Regul. Integr. Comp. Physiol.* **284**, R1-R12.
Forster, C., Silwedel, C., Golenhofen, N., Burek, M., Kietz, S., Mankertz, J. and Drenckhahn, D. (2005). Occludin as direct target for glucocorticoid-induced improvement of blood-brain barrier properties in a murine in vitro system. *J. Physiol.* **565**, 475-486.
Funder, J. W. (2005). The nongenomic actions of aldosterone. *Endocr. Rev.* **26**, 313-321.
Funder, J. W., Pearce, P. T., Smith, R. and Smith, A. I. (1988). Mineralocorticoid action: target tissue specificity is enzyme, not receptor, mediated. *Science* **242**, 583-585.
Gates, P. E., Tanaka, H., Hiatt, W. R. and Seals, D. R. (2004). Dietary sodium restriction rapidly improves large elastic artery compliance in older adults with systolic hypertension. *Hypertension* **44**, 35-41.
Goerge, T., Niemeyer, A., Rogge, P., Ossig, R., Oberleithner, H. and Schneider, S. W. (2002). Secretion pores in human endothelial cells during acute hypoxia. *J. Membr. Biol.* **187**, 203-211.
Golestaneh, N., Klein, C., Valamanesh, F., Suarez, G., Agarwal, M. K. and Mirshahi, M. (2001). Mineralocorticoid receptor-mediated signaling regulates the ion gated sodium channel in vascular endothelial cells and requires an intact cytoskeleton. *Biochem. Biophys. Res. Commun.* **280**, 1300-1306.
Hadoke, P. W., Christy, C., Kotelevtsev, Y. V., Williams, B. C., Kenyon, C. J., Seckl, J. R., Mullins, J. J. and Walker, B. R. (2001). Endothelial cell dysfunction in mice after transgenic knockout of type 2, but not type 1, 11beta-hydroxysteroid dehydrogenase. *Circulation* **104**, 2832-2837.
Henderson, R. M., Schneider, S., Li, Q., Hornby, D., White, S. J. and Oberleithner, H. (1996). Imaging ROMK1 inwardly rectifying ATP-sensitive K+ channel protein using atomic force microscopy. *Proc. Natl. Acad. Sci. USA* **93**, 8756-8760.
Hoh, J. H. and Schoenenberger, C.-A. (1994). Surface morphology and mechanical properties of MDCK monolayers by atomic force microscopy. *J. Cell Sci.* **107**, 1105-1114.
Hughey, R. P., Mueller, G. M., Bruns, J. B., Kinlough, C. L., Poland, P. A., Harkleroad, K. L., Carattino, M. D. and Kleyman, T. R. (2003). Maturation of the epithelial Na+ channel involves proteolytic processing of the alpha- and gamma-subunits. *J. Biol. Chem.* **278**, 37073-37082.
Jaffe, E. A., Nachman, R. L., Becker, C. G. and Minick, C. R. (1973). Culture of human endothelial cells derived from umbilical veins. Identification by morphologic and immunologic criteria. *J. Clin. Invest.* **52**, 2745-2756.
Kataoka, N., Iwaki, K., Hashimoto, K., Mochizuki, S., Ogasawara, Y., Sato, M., Tsujioka, K. and Kajiya, F. (2002). Measurements of endothelial cell-to-cell and cell-to-substrate gaps and micromechanical properties of endothelial cells during monocyte adhesion. *Proc. Natl. Acad. Sci. USA* **99**, 15638-15643.
Krug, A. W., Grossmann, C., Schuster, C., Freudinger, R., Mildenberger, S., Govindan, M. V. and Gekle, M. (2003). Aldosterone stimulates epidermal growth factor receptor expression. *J. Biol. Chem.* **278**, 43060-43066.
Lacolley, P., Labat, C., Pujol, A., Delcayre, C., Benetos, A. and Safar, M. (2002).

Increased carotid wall elastic modulus and fibronectin in aldosterone-salt-treated rats: effects of eplerenone. *Circulation* **106**, 2848-2853.

Lombes, M., Oblin, M. E., Gasc, J. M., Baulieu, E. E., Farman, N. and Bonvalet, J. P. (1992). Immunohistochemical and biochemical evidence for a cardiovascular mineralocorticoid receptor. *Circ. Res.* **71**, 503-510.

Minami, T. and Aird, W. C. (2005). Endothelial cell gene regulation. *Trends Cardiovasc. Med.* **15**, 174-184.

Muller, A. M., Hermanns, M. I., Cronen, C. and Kirkpatrick, C. J. (2002). Comparative study of adhesion molecule expression in cultured human macro- and microvascular endothelial cells. *Exp. Mol. Pathol.* **73**, 171-180.

Oberleithner, H. (2005). Aldosterone makes human endothelium stiff and vulnerable. *Kidney Int.* **67**, 1680-1682.

Oberleithner, H., Schneider, S. W. and Henderson, R. M. (1997). Structural activity of a cloned potassium channel (ROMK1) monitored with the atomic force microscope: the "molecular-sandwich" technique. *Proc. Natl. Acad. Sci. USA* **94**, 14144-14149.

Oberleithner, H., Schneider, S. W., Albermann, L., Hillebrand, U., Ludwig, T., Riethmuller, C., Shahin, V., Schafer, C. and Schillers, H. (2003). Endothelial cell swelling by aldosterone. *J. Membr. Biol.* **196**, 163-172.

Oberleithner, H., Ludwig, T., Riethmuller, C., Hillebrand, U., Albermann, L., Schafer, C., Shahin, V. and Schillers, H. (2004). Human endothelium: target for aldosterone. *Hypertension* **43**, 952-956.

Palmer, L. G. and Frindt, G. (2000). Aldosterone and potassium secretion by the cortical collecting duct. *Kidney Int.* **57**, 1324-1328.

Palmieri, E. A., Biondi, B. and Fazio, S. (2002). Aldosterone receptor blockade in the management of heart failure. *Heart Fail. Rev.* **7**, 205-219.

Pfister, G., Stroh, C. M., Perschinka, H., Kind, M., Knoflach, M., Hinterdorfer, P. and Wick, G. (2005). Detection of HSP60 on the membrane surface of stressed human endothelial cells by atomic force and confocal microscopy. *J. Cell Sci.* **118**, 1587-1594.

Pitt, B., Remme, W., Zannad, F., Neaton, J., Martinez, F., Roniker, B., Hurley, S., Kleiman, J. and Gaitlin, M. (2003). Eplerenone, a selective aldosterone blocker, in patients with left ventricular dysfunction after myocardial infarction. *N. Engl. J. Med.* **348**, 1309-1321.

Radmacher, M., Fritz, M., Kacher, C. M., Cleveland, J. P. and Hansma, P. K. (1996). Measuring the viscoelastic properties of human platelets with the atomic force microscope. *Biophys. J.* **70**, 556-567.

Rajagopalan, S., Duquaine, D., King, S., Pitt, B. and Patel, P. (2002). Mineralocorticoid receptor antagonism in experimental atherosclerosis. *Circulation* **105**, 2212-2216.

Robert-Nicoud, M., Flahaut, M., Elalouf, J. M., Nicod, M., Salinas, M., Bens, M., Doucet, A., Wincker, P., Artiguenave, F., Horisberger, J. D. et al. (2001). Transcriptome of a mouse kidney cortical collecting duct cell line: effects of aldosterone and vasopressin. *Proc. Natl. Acad. Sci. USA* **98**, 2712-2716.

Romero, I. A., Radewicz, K., Jubin, E., Michel, C. C., Greenwood, J., Couraud, P. O. and Adamson, P. (2003). Changes in cytoskeletal and tight junctional proteins correlate with decreased permeability induced by dexamethasone in cultured rat brain endothelial cells. *Neurosci. Lett.* **344**, 112-116.

Schafer, J. A. (2002). Abnormal regulation of ENaC: syndromes of salt retention and salt wasting by the collecting duct. *Am. J. Physiol. Renal Physiol.* **283**, F221-F235.

Schneider, S. W., Pagel, P., Rotsch, C., Danker, T., Oberleithner, H., Radmacher, M. and Schwab, A. (2000). Volume dynamics in migrating epithelial cells measured with atomic force microscopy. *Pflugers Arch.* **439**, 297-303.

Schneider, S. W., Matzke, R., Radmacher, M. and Oberleithner, H. (2004). Shape and volume of living aldosterone-sensitive cells imaged with the atomic force microscope. *Methods Mol. Biol.* **242**, 255-279.

Stier, C. T., Jr, Chander, P. N. and Rocha, R. (2002). Aldosterone as a mediator in cardiovascular injury. *Cardiol. Rev.* **10**, 97-107.

Tanaka, N., Kawasaki, K., Nejime, N., Kubota, Y., Nakamura, K., Kunitomo, M., Takahashi, K., Hashimoto, M. and Shinozuka, K. (2004). P2Y receptor-mediated Ca(2+) signaling increases human vascular endothelial cell permeability. *J. Pharmacol. Sci.* **95**, 174-180.

Tiruppathi, C., Malik, A. B., Del Vecchio, P. J., Keese, C. R. and Giaever, I. (1992). Electrical method for detection of endothelial cell shape change in real time: assessment of endothelial barrier function. *Proc. Natl. Acad. Sci. USA* **89**, 7919-7923.

Underwood, J. L., Murphy, C. G., Chen, J., Franse-Carman, L., Wood, I., Epstein, D. L. and Alvarado, J. A. (1999). Glucocorticoids regulate transendothelial fluid flow resistance and formation of intercellular junctions. *Am. J. Physiol.* **277**, C330-C342.

Vigne, P., Champigny, G., Marsault, R., Barbry, P., Frelin, C. and Lazdunski, M. (1989). A new type of amiloride-sensitive cationic channel in endothelial cells of brain microvessels. *J. Biol. Chem.* **264**, 7663-7668.

Wegener, J., Keese, C. R. and Giaever, I. (2000). Electric cell-substrate impedance sensing (ECIS) as a noninvasive means to monitor the kinetics of cell spreading to artificial surfaces. *Exp. Cell Res.* **259**, 158-166.